International Journal of Thermal Sciences 48 (2009) 1081–1093

Contents lists available at ScienceDirect

International Journal of Thermal Sciences

www.elsevier.com/locate/ijts

Two-dimensional non-linear inverse heat conduction problem based on the singular value decomposition

Juan Andrés Martín García [a,1], José María Gutiérrez Cabeza [b,*,2], Alfonso Corz Rodríguez [c,3]

[a] Department of Electrical Engineering, University of Cádiz, Escuela Politécnica Superior de Algeciras, Avda. Ramón Puyol, s/n, 11202 Algeciras, Cádiz, Spain
[b] Department of Applied Physics, University of Cádiz, Escuela Politécnica Superior de Algeciras, Avda. Ramón Puyol, s/n, 11202 Algeciras, Cádiz, Spain
[c] Department of Industrial and Civil Engineering, University of Cádiz, Escuela Politécnica Superior de Algeciras, Avda. Ramón Puyol, s/n, 11202 Algeciras, Cádiz, Spain

ARTICLE INFO

Article history:
Received 18 July 2007
Received in revised form 11 September 2008
Accepted 11 September 2008
Available online 30 September 2008

Keywords:
Inverse heat conduction
Singular value decomposition
Function specification method

ABSTRACT

In this paper an efficient sequential method is developed in order to estimate the unknown boundary condition on the surface of a body from transient temperature measurements inside the solid. This numerical approach for solving an inverse heat conduction problem (IHCP) takes into account two-dimensional problems, planar or axisymmetric cylindrical, composite materials with irregular boundaries and temperature-dependent thermal properties. The unknown surface condition is assumed to have abrupt changes at unknown times. The regularization procedure used for the solution of the IHCP is based on the singular value decomposition technique. An overall estimate of error is defined in order to find the optimal estimation in the 2D IHCP (linear and non-linear). The stability and accuracy of the scheme presented is evaluated by comparison with the Function Specification Method. This comparative study has been carried out using numerically simulated data, and the parameters considered include shape of input, noise level of measurement, size of time step and temperature-dependent thermal properties. A good agreement was found between both methods. Beside this, the slight differences on estimations and number of future temperatures are discussed in this paper.

1. Introduction

Several functions and parameters can be estimated from the inverse heat conduction problem (IHCP): static and moving heating sources, material properties, initial conditions, boundary conditions, etc. This study is confined to the estimation of an unknown boundary condition. The unknown function can be a surface flux, a surface temperature or a heat transfer coefficient. The lack of information is usually due to the difficulty of installing sensors in the boundary. This circumstance appears in applications where the boundary is inaccessible [1,2], in simulation of space vehicle re-entry [3], in metallurgic applications [4,5], etc. In order to recover the unknown time history, it is necessary to obtain the additional information provided by remote temperature sensors placed at interior locations.

It is well known that the IHCP is an ill-posed problem because small errors in the data might induce large errors in the computed solution. As a consequence of the diffusive nature of heat flow, the thermal response at some distance of the boundary is damped and lagged with respect to the active input at the boundary. This implies that in many cases the inverse problem presents a low or insufficient sensitivity. On the other hand, in linear problems the relationship between the thermal response and the unknown input can be expressed through a sensitivity matrix which tends to be quasi-singular. This fact explains the principal difficulty of the IHCP: the estimation tends to be unstable due to the great amplification of measurements errors. This difficulty is increased when the time interval between measurements is reduced. The influence of the most important factors in this problem can be discussed considering the exact solution of Burggraf [6]. For this reason, special techniques are needed in order to restore stability. Moreover, the numerical difficulties increase substantially with the dimensionality and the non-linearity of the inverse problem. Thus, an efficient as well as reliable method is essential for it to be applicable to real-world problems.

Fortunately, many methods have been reported to solve IHCPs. Among the most versatile methods (applicable to solve multidimensional and non-linear IHCP), the following can be mentioned: Tikhonov regularization [7], iterative regularization [8], mollification [9], and the function specification method (FSM) [6]. The first two methods are usually considered as "whole domain" because all measured temperature data are used in order to simultaneously estimate all the components of the unknown input. By contrast,

* Corresponding author.
E-mail addresses: juanandres.martin@uca.es (J.A.M. García), josemaria.gutierrez@uca.es (J.M.G. Cabeza), alfonso.corz@uca.es (A.C. Rodríguez).
[1] Tel.: +34 956 028167; fax: +34 956 028001.
[2] Tel.: +34 956 028031; fax: +34 956 028001.
[3] Tel.: +34 952 137045; fax: +34 952 137045.

1290-0729/$ – see front matter
doi:10.1016/j.ijthermalsci.2008.09.002

Nomenclature

C	constant	
c	specific heat	J/kg °C
$\mathbf{H}$	partition of sensitivity matrix	
h	heat transfer coefficient	W/m^2 °C
J	number of temperature sensors	
k	thermal conductivity	W/m °C
M	total number of time steps	
m	present time step	
N	number of estimated values during τ	
$\mathbf{n}$	inwards normal vector	
P	number of spatial heat flux parameters	
p	reduced rank	
$\mathbf{q}$	heat flux vector	
q	heat flux	W/m^2
r	number of future time steps and cylindrical coordinate	m
$\mathbf{S}$	diagonal matrix	
S	overall estimate of error	W/m^2
s	surface coordinate	m
$\mathbf{T}$	vector of calculated temperatures	
T	temperature	°C
t	time	s
$\mathbf{U}$	orthogonal matrix	
$\mathbf{u}$	left singular vector	
u	Gaussian random numbers (normalized)	
$\mathbf{V}$	orthogonal matrix	
$\mathbf{v}$	right singular vector	
$\mathbf{X}$	sensitivity matrix	
$\mathbf{Y}$	vector of measured temperatures	
Y	measured temperature	°C
z	cylindrical coordinate	m

Greek symbols

Γ	boundary	
Δt	time step size	s
$\Delta\phi$	response to a unit pulse	°C/W m^{-2}
ε	random error	
λ	singular value	
ϕ	response to a unit step change	°C/W m^{-2}
ρ	density	kg/m^3
σ	standard deviation	°C
τ	temporal interval	
Φ	basis function	
Ω	domain	

Subscripts

0	initial value
fut	future components
i	time index
j	sensor index
k	parameter index
past	previous components
r	in direction of r-axis
red	reduced rank approximation
z	in direction of z-axis

Superscripts

T	transposed
$\wedge$	estimated
$*$	arbitrary

the last two methods are sequential and hence, only a little part of available measurement is used in each step and only one component of the unknown input is estimated at each step. This fact can be an advantage in an on-line process.

For unsteady problems, the FSM developed by Beck et al. [6] has been widely used, combined with any of those above mentioned whole domain methods. The combination of the Tikhonov regularization method [7] and the sequential FSM has already been implemented for two-dimensional and non-linear IHCPs [10]. In addition, it must be mentioned that the combination of the gradient method [8] and the sequential FSM has also been investigated for one and two-dimensional IHCPs. Dowding and Beck [11] addressed a sequential gradient method for two-dimensional IHCPs with and without function specification, additionally using the conventional regularization method.

Another effective technique to solve ill-posed problems is based on the singular value decomposition (SVD) of an ill-conditioned matrix [12] and posterior truncation of singular values. The truncated SVD method has been applied to solve inverse problem in steady [13,14] and transient heat conduction [15,16]. The stabilizing effect of this method is based on the elimination of the smallest singular values of the sensitivity matrix (and the corresponding left and right singular vectors), so that p largest singular values are only considered. This procedure implies a reduction of the matrix rank. The new rank of the truncated sensitivity matrix is p. This reduced rank approximation reduces the condition number and the numerical instability. More recently, Shenefelt [17] presented the data filtering interpretation by the truncated SVD in IHCP. In all these previous studies, the truncated SVD method was applied as a whole domain procedure. Recently, the truncated SVD method has also been applied in a sequential form [18,19]. In similar way to the classical sequential methods, the sequential algorithm uses only a reduced number of future temperatures in each step (r). As well as this, the truncated SVD is applied to a small sensitivity matrix.

Gutiérrez et al. [19] compare the sequential SVD method with the standard whole domain SVD for one-dimensional and linear problems. The sequential SVD algorithm presents two tunable hyperparameters: the number of future temperature (r) and the rank of the truncated sensitivity matrix (p). In accordance with the data filtering interpretation of Shenefelt [17], the principal regularization effect is carried out by the reduced rank p. This implies the elimination of the band-pass filters centred on high frequencies, which corresponding to random noise. Furthermore, the sequential SVD algorithm allows controlling the wideband with the number of future temperature r.

Lagier et al. [18] have presented the sequential SVD method for solving the general linear multidimensional unsteady inverse heat conduction problem. This numerical method is based on the Boundary Element Method formulation.

In this paper, the sequential SVD method is investigated for the two-dimensional (using Cartesian or axisymmetric cylindrical coordinates) and non-linear IHCP in irregular-shaped bodies with temperature-dependent thermal properties. This study is a generalization of previous work of Gutiérrez et al. [19]. The numerical method is based on the Finite Element Method (FEM) formulation. The sequential SVD technique is capable of estimating space and time-varying surface heat flux. The unknown surface condition is assumed to have abrupt changes at unknown times. In addition, the sequential form of this method allows the use of a quasi-linear approximation in the calculations of temperatures and sensitivity coefficients [6,10]. This fact results in an efficient scheme (the

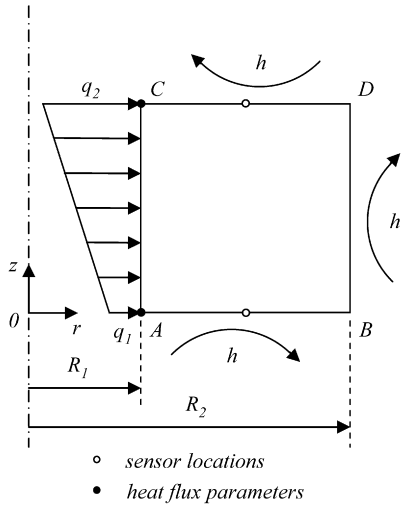

Fig. 1. Geometry, coordinates and sensor locations of the sample problem.

computer time is substantially reduced) because iteration is not required for non-linear problems.

The stability and accuracy of the method are demonstrated by several numerical examples based on strict standard tests, and the results are compared to an existing regularization method such as the well known FSM. In this comparison, the simplest model of function specification is considered (a constant heat flux functional form) with no additional regularization procedure. In this case, numerically simulated data have been used. In this study the parameters considered have been the following: shape of the input (four tests with different shapes are used), noise level of measurement, size of time step and temperature-dependent thermal properties. The thermo-physical properties are assumed as constant values for the linear problem. In the non-linear problem, a linear dependence of thermal conductivity (with the temperature) has been chosen, while the remaining properties are assumed as constant values for simplicity and without loss of generality.

The contents of this paper are briefly outlined below. In Section 2, the mathematical description of the problem is presented. In Section 3, the regularization procedure used to solve the inverse problem is developed. Numerical examples are discussed in Section 4. Finally, the conclusions are exposed in Section 5.

2. Problem description

Without loss of generality and in order to illustrate the method, the following transient heat conduction problem is considered. The sample body is an axisymmetric cylinder wall with temperature-dependent thermal properties. The spatial domain is Ω and the symbols Γ_1 and Γ_2 represent the domain boundaries. Fig. 1 shows a schema of the geometry and the coordinates for a two-dimensional axisymmetric cylindrical body considered with its boundary conditions. Note that Γ_1 is the boundary AC (see Fig. 1) and Γ_2 is the convective boundary ABDC (AB, BD and DC).

The mathematical formulation of the corresponding problem is stated as follows:

$$\frac{1}{r}\frac{\partial}{\partial r}\left(kr\frac{\partial T}{\partial r}\right)+\frac{\partial}{\partial z}\left(k\frac{\partial T}{\partial z}\right)=\rho c\frac{\partial T}{\partial t},\quad (r,z)\in\Omega,\ 0\leqslant t\leqslant t_M \tag{1a}$$

$$-k\frac{\partial T}{\partial r}n_r-k\frac{\partial T}{\partial z}n_z=q(r,z,t),\quad (r,z)\in\Gamma_1,\ 0\leqslant t\leqslant t_M \tag{1b}$$

$$-k\frac{\partial T}{\partial r}n_r-k\frac{\partial T}{\partial z}n_z=h\left[T_\infty-T(r,z,t)\right]\quad (r,z)\in\Gamma_2,\ 0\leqslant t\leqslant t_M \tag{1c}$$

$$T(r,z,0)=T_0(r,z),\quad (r,z)\in\Omega,\ t=0 \tag{1d}$$

where Eq. (1a) is the two-dimensional heat conduction equation for axisymmetric cylindrical coordinates (r,z). The boundary condition in Eq. (1c) represents a convective boundary condition (third kind), but even boundary conditions of the first and second kinds can be considered in the boundary Γ_2. The geometry, thermal properties (k,ρ,c), boundary conditions (h,T_∞), and the initial condition (T_0) are assumed to be known completely. In the direct problem, the heat flux $q(r,z,t)$ in Eq. (1b) represents a flux imposed in the boundary Γ_1. In the inverse problem, $q(r,z,t)$ will be the unknown function to be estimated. This flux can be an arbitrary function. The symbols n_r and n_z are r- and z-components of the normal unitary vector, **n**, to the boundary surface which is pointing towards inside of the body. Hence, the heat flux, $q(r,z,t)$, penetrating in the solid through a surface is positive.

In the numerical simulation of this study, four different functions (test cases) will be considered. The response of the direct problem, $T(r,z,t)$, will be calculated numerically using FEM formulation. We are interested in the response at sensors locations, because in the commonly accepted definition of the IHCP, the reconstruction of the unknown function, $q(r,z,t)$ is carried out from discrete temperature measurements at these internal positions. Let measurements, $Y_{ji}=Y(r_j,z_j,t_i)$, be taken at sensor j $(j=1,2,\ldots,J)$ for times t_i, where $i=1,2,\ldots,M$. As the measured temperatures Y_{ji} are affected by errors, they are simulated using the numerical values of the temperature calculated in the direct problem, $T_{ji}=T(r_j,z_j,t_i)$, for times $t_i=i\Delta t$ (the time intervals of the measurements) at each sensor j. Then, random errors ε_{ji} are added according to: $Y_{ji}=T_{ji}+\varepsilon_{ji}$, where $\varepsilon_{ji}=Cu_{ji}$. Random numbers u_{ji} have been obtained using a random generator according to a normal (or Gaussian) distribution with zero mean, uncorrelated and unit standard deviation. The constant C is chosen, so that $C=\sigma$, where σ is the standard deviation of measured temperatures.

3. Inverse problem

In the inverse problem solution method, firstly the domain is divided into finite elements, and secondly the discretization, over time and space, of the unknown surface heat flux, $q(r,z,t)$ in Eq. (1b), must be done. These approximations are carried out in the same way as Osman et al. [10] have made, and they are summarized below.

If a surface coordinate "s" is introduced, the surface heat flux in Eq. (1b) can be expressed as:

$$q(r,z,t)=q(s,t),\quad (r,z)\in\Gamma_1 \tag{2}$$

where s is the surface coordinate along boundary Γ_1.

Boundary Γ_1 is divided into sub-intervals and the spatial approximation of $q(s,t)$ along this boundary, at a fixed time instant, is made using P interpolating functions, $\Phi_k(s)$, with $k=1,2,\ldots,P$, which approximate the function $q(s,t)$ over each surface segment in Γ_1 using the values of the heat flux at the P surface parameter nodes,

$$q(s,t)=\sum_{k=1}^{P}\Phi_k(s)q_k(t) \tag{3}$$

where P is the total number of spatial parameter nodes, and $\Phi_k(s)$ are the basis functions for interpolating. The function $q_k(t)=q(s_k,t)$ in Eq. (3) represents the heat flux history at the kth parameter node. In this way, the selected parameters are interpolated at all the surface nodes.

Now, the approximation of the temporal distribution of the surface heat flux is carried out by discretizing the continuous function $q_k(t)$ in Eq. (3). The given time interval, $0\leqslant t\leqslant t_M$, is usually divided into uniform sub-intervals, each of size $\Delta t=t_M/M$, with

$t_i = i\Delta t$, where $i = 1, 2, \ldots, M$. The function $q_k(t)$ at the spatial location s_k is approximated by a piecewise constant function on time by

$$q_k(t) = (q_{k1}, q_{k2}, \ldots, q_{ki}, \ldots, q_{kM}) \tag{4}$$

where $q_{ki} = q_k(t_i)$ is the value of the arbitrary surface heat flux function at the kth parameter location and at time t_i, which is centred at the middle of the time step ($t_{i-1/2}$).

Therefore, the global approximation of the surface heat flux at time t_i is given by

$$q(s, t_i) = \sum_{k=1}^{P} \Phi_k(s) q_{ki} \tag{5}$$

Flux components q_{ki} are the unknown surface heat flux parameters to be calculated. These parameters q_{ki} are estimated simultaneously in space, index k, and sequentially in time, index i. The discretization of the surface heat flux, $q(s, t)$, over time and space, involves the following parameters:

$$\mathbf{q} = (\mathbf{q}_1, \mathbf{q}_2, \ldots, \mathbf{q}_k, \ldots, \mathbf{q}_P)^T \tag{6a}$$

with

$$\mathbf{q}_k = (q_{k1}, q_{k2}, \ldots, q_{ki}, \ldots, q_{kM})^T \tag{6b}$$

The aim of the inverse problem is to estimate the components q_{ki}, with $k = 1, 2, \ldots, P$ and $i = 1, 2, \ldots, M$ using, as additional information, the discrete temperature measurements Y_{ji}, with $j = 1, 2, \ldots, J$ and $i = 1, 2, \ldots, M$, which are taken at interior positions of the solid.

3.1. Standard form for the 2D linear IHCP

The purpose of this subsection is to obtain the well-known temperature equations called standard form for the linear IHCP [6] when two-dimensional problems are considered. The discussion in this subsection is confined to the linear IHCP but nearly the same approach can be used for the quasi-linear analysis which is discussed in Subsection 3.3. The analysis can be performed using either algebraic or matrix notation but the latter analysis is preferred because it is more compact and general. The structure of vectors and matrices will be detailed later in this paper.

In a linear problem, a linear dependency exists between the input, in this case $q(r, z, t)$, and the response, $T(r, z, t)$, at sensors locations. This dependency can be expressed analytically by the Duhamel integral in a discrete form:

$$T_{jM} = T_{j0} + \sum_{k=1}^{P} \sum_{i=1}^{M} q_{ki} \Delta\phi_{kj(M-i)} \tag{7}$$

where $T_{jM} = T(r_j, z_j, t_M)$ is the value of the temperature response at the jth sensor location and at time t_M, T_{j0} is the initial condition at the jth sensor location, $\phi_{kji} = \phi_k(r_j, z_j, t_i)$ represents the temperature response at the jth sensor location, at time t_i, for a unit step change of the surface heat flux kth parameter, and hence $\Delta\phi_{kji} = \phi_{kj(i+1)} - \phi_{kji}$ represents the temperature response to a unit pulse on the surface heat flux kth parameter, at the jth sensor location and at time t_i. Consequently, $\Delta\phi_{kji}$ represents the pulse sensitivity coefficient measured at location (r_j, z_j) and at time t_i with respect to the surface heat flux kth parameter. Eq. (7) represents the convolution between the set of parameters $(q_{k1}, q_{k2}, \ldots, q_{kM})$ and the sensitivity coefficients $(\Delta\phi_{kj(M-1)}, \Delta\phi_{kj(M-2)}, \ldots, \Delta\phi_{kj0})$ with $k = 1, 2, \ldots, P$.

Considering Eq. (7) for $M = 1, 2, \ldots$, it is possible to obtain the following matrix equation:

$$\mathbf{T} = [\mathbf{X}]\mathbf{q} + \mathbf{T}_0 \tag{8}$$

where $\mathbf{T}$ is the vector of temperature response at each one of the sensors, $\mathbf{q}$ is the heat flux vector given by Eqs. (6a), (6b), $[\mathbf{X}]$ is the sensitivity matrix and $\mathbf{T}_0$ is the temperature vector corresponding to the initial condition. The $\mathbf{T}$ temperature vector can be expressed as:

$$\mathbf{T} = (\mathbf{T}_1, \mathbf{T}_2, \ldots, \mathbf{T}_j, \ldots, \mathbf{T}_J)^T \tag{9a}$$

with

$$\mathbf{T}_j = (T_{j1}, T_{j2}, \ldots, T_{ji}, \ldots, T_{jM})^T \tag{9b}$$

the $[\mathbf{X}]$ sensitivity matrix is:

$$[\mathbf{X}] = \begin{bmatrix} \mathbf{X}_{11} & \mathbf{X}_{12} & \cdots & \mathbf{X}_{1k} & \cdots & \mathbf{X}_{1P} \\ \mathbf{X}_{21} & \mathbf{X}_{22} & \cdots & \mathbf{X}_{2k} & \cdots & \mathbf{X}_{2P} \\ \vdots & \vdots & \ddots & \vdots & \cdots & \vdots \\ \mathbf{X}_{j1} & \mathbf{X}_{j2} & \cdots & \mathbf{X}_{jk} & \cdots & \mathbf{X}_{jP} \\ \vdots & \vdots & \ddots & \vdots & \ddots & \vdots \\ \mathbf{X}_{J1} & \mathbf{X}_{J2} & \cdots & \mathbf{X}_{Jk} & \cdots & \mathbf{X}_{JP} \end{bmatrix} \tag{9c}$$

with each $[\mathbf{X}_{jk}]$ sub-matrix expressed as:

$$[\mathbf{X}_{jk}] = \begin{bmatrix} \Delta\phi_{kj0} & 0 & \cdots & 0 & \cdots & 0 \\ \Delta\phi_{kj1} & \Delta\phi_{kj0} & \cdots & 0 & \cdots & 0 \\ \vdots & \vdots & \ddots & \vdots & \cdots & \vdots \\ \Delta\phi_{kj(i-1)} & \Delta\phi_{kj(i-2)} & \cdots & \Delta\phi_{kj0} & \cdots & 0 \\ \vdots & \vdots & \vdots & \vdots & \ddots & \vdots \\ \Delta\phi_{kj(M-1)} & \Delta\phi_{kj(M-2)} & \cdots & \Delta\phi_{kj(M-i)} & \cdots & \Delta\phi_{kj0} \end{bmatrix} \tag{9d}$$

and the initial temperature vector $\mathbf{T}_0$ is:

$$\mathbf{T}_0 = (\mathbf{T}_{10}, \mathbf{T}_{20}, \ldots, \mathbf{T}_{j0}, \ldots, \mathbf{T}_{J0})^T \tag{9e}$$

where $\mathbf{T}_{j0}$ sub-vector ($(M \times 1)$ in dimension) contains the initial temperature T_{j0} at the jth sensor location

$$\mathbf{T}_{j0} = T_{j0}(1, 1, \ldots, 1, \ldots, 1)^T \tag{9f}$$

If the time history covers a long period of time, the $[\mathbf{X}]$ matrix and the corresponding vectors can be of a considerable dimension. In Eq. (9d), $[\mathbf{X}_{jk}]$ is a square matrix ($M \times M$). This matrix is called the pulse sensitivity coefficient matrix for $\mathbf{q}_k$. Its structure is lower triangular with $\Delta\phi_{kj0}$'s along the main diagonal, $\Delta\phi_{kj1}$'s along the diagonal just below the main one, and so on. Therefore, in Eq. (9c), the $[\mathbf{X}]$ matrix is $(J \times M) \times (P \times M)$ in dimensions. Additionally, $\mathbf{T}$, $\mathbf{T}_0$ and $\mathbf{q}$ vectors are $(J \times M)$, $(J \times M)$ and $(P \times M)$ in dimensions respectively. Note that if the number of sensors (J) is considered equal to the number of parameters (P) to estimate (components of the surface heat flux), the $[\mathbf{X}]$ matrix, in Eq. (8), is also a square matrix, and $\mathbf{T}$ and $\mathbf{q}$ vectors are equal in dimensions. Then, the first attempt in order to solve the inverse problem can be the identification of measured temperatures Y_{ji} with the calculated temperatures T_{ji}, expressed by Eq. (8), so that the unknown vector $\mathbf{q}$ can be obtained from:

$$\mathbf{q} = [\mathbf{X}]^{-1}(\mathbf{Y} - \mathbf{T}_0) \tag{10}$$

We note that diagonal coefficients of $[\mathbf{X}_{jk}]$, in Eq. (9d), are equal to $\Delta\phi_{kj0}$. This sensitivity coefficient represents the response (at the jth sensor location) to a unitary pulse on the surface heat flux kth component (with a wideness of one time step), just when the pulse has finished. If the time step is sufficiently small, this response can be several orders of magnitude lower than others sensitivity values. This justifies (from a physical point of view) that $[\mathbf{X}]$ is an ill-conditioned matrix. On the other hand, as Y_{ji} is affected by measurements errors, the estimation of $\mathbf{q}$ by Eq. (10) will be unstable.

In the sequential IHCP methods based on a march ahead in time, the heat flux components, $q_{k1}, q_{k2}, \ldots, q_{k(m-1)}$, of each $\mathbf{q}_k$ vector, are considered previously estimated and they are denoted $\hat{q}_{k1}, \hat{q}_{k2}, \ldots, \hat{q}_{k(m-1)}$. Estimates of the components q_{km} for $k = 1, 2, \ldots, P$, corresponding to the m-time step (located in the time interval between t_{m-1} and t_m) are needed. In order to obtain the sequential algorithm SVD, Eq. (8) is considered and it is extended to r future time steps from the last estimated component (component $m-1$). In a partitioned form, the matrix equation can be written as:

$$\begin{bmatrix} T_{1\,\mathrm{past}} \\ T_{1\,\mathrm{fut}} \\ \vdots \\ T_{J\,\mathrm{past}} \\ T_{J\,\mathrm{fut}} \end{bmatrix} = \begin{bmatrix} \mathbf{X}_{11\,\mathrm{past}} & \mathbf{0} & \cdots & \mathbf{X}_{1P\,\mathrm{past}} & \mathbf{0} \\ \mathbf{H}_{11} & \mathbf{X}_{11\,\mathrm{fut}} & \cdots & \mathbf{H}_{1P} & \mathbf{X}_{1P\,\mathrm{fut}} \\ \vdots & \vdots & \ddots & \vdots & \vdots \\ \mathbf{X}_{J1\,\mathrm{past}} & \mathbf{0} & \cdots & \mathbf{X}_{JP\,\mathrm{past}} & \mathbf{0} \\ \mathbf{H}_{J1} & \mathbf{X}_{J1\,\mathrm{fut}} & \cdots & \mathbf{H}_{JP} & \mathbf{X}_{JP\,\mathrm{fut}} \end{bmatrix} \begin{bmatrix} \hat{\mathbf{q}}_{1\,\mathrm{past}} \\ \mathbf{q}_{1\,\mathrm{fut}} \\ \vdots \\ \hat{\mathbf{q}}_{P\,\mathrm{past}} \\ \mathbf{q}_{P\,\mathrm{fut}} \end{bmatrix} + \begin{bmatrix} T_{10\,\mathrm{past}} \\ T_{10\,\mathrm{fut}} \\ \vdots \\ T_{J0\,\mathrm{past}} \\ T_{J0\,\mathrm{fut}} \end{bmatrix} \tag{11}$$

where the vectors are:

$$\mathbf{T}_{j\,\mathrm{past}} = (T_{j1}, T_{j2}, \ldots, T_{j(m-1)})^T \tag{12a}$$

$$\mathbf{T}_{j\,\mathrm{fut}} = (T_{jm}, T_{j(m+1)}, \ldots, T_{j(m+i-1)}, \ldots, T_{j(m+r-1)})^T \tag{12b}$$

$$\hat{\mathbf{q}}_{k\,\mathrm{past}} = (\hat{q}_{k1}, \hat{q}_{k2}, \ldots, \hat{q}_{k(m-1)})^T \tag{12c}$$

$$\mathbf{q}_{k\,\mathrm{fut}} = (q_{km}, q_{k(m+1)}, \ldots, q_{k(m+i-1)}, \ldots, q_{k(m+r-1)})^T \tag{12d}$$

and the sub-matrices, in Eq. (11), are:

$$[\mathbf{X}_{jk\,\mathrm{past}}] = \begin{bmatrix} \Delta\phi_{kj0} & 0 & \cdots & 0 \\ \Delta\phi_{kj1} & \Delta\phi_{kj0} & \cdots & 0 \\ \vdots & \vdots & \ddots & \vdots \\ \Delta\phi_{kj(m-2)} & \Delta\phi_{kj(m-3)} & \cdots & \Delta\phi_{kj0} \end{bmatrix} \tag{12e}$$

$$[\mathbf{H}_{jk}] = \begin{bmatrix} \Delta\phi_{kj(m-1)} & \Delta\phi_{kj(m-2)} & \cdots & \Delta\phi_{kj1} \\ \Delta\phi_{kjm} & \Delta\phi_{kj(m-1)} & \cdots & \Delta\phi_{kj2} \\ \vdots & \vdots & \ddots & \vdots \\ \Delta\phi_{kj(m+r-2)} & \Delta\phi_{kj(m+r-3)} & \cdots & \Delta\phi_{kjr} \end{bmatrix} \tag{12f}$$

$$[\mathbf{X}_{jk\,\mathrm{fut}}] = \begin{bmatrix} \Delta\phi_{kj0} & 0 & \cdots & 0 & \cdots & 0 \\ \Delta\phi_{kj1} & \Delta\phi_{kj0} & \cdots & 0 & \cdots & 0 \\ \vdots & \vdots & \ddots & \vdots & \cdots & \vdots \\ \Delta\phi_{kj(i-1)} & \Delta\phi_{kj(i-2)} & \cdots & \Delta\phi_{kj0} & \cdots & 0 \\ \vdots & \vdots & \vdots & \vdots & \ddots & \vdots \\ \Delta\phi_{kj(r-1)} & \Delta\phi_{kj(r-2)} & \cdots & \Delta\phi_{kj(r-i)} & \cdots & \Delta\phi_{kj0} \end{bmatrix} \tag{12g}$$

It should be noted that $\mathbf{T}_{j0\,\mathrm{past}}$ and $\mathbf{T}_{j0\,\mathrm{fut}}$ vectors contain the same information (initial temperature T_{j0} at the jth sensor location), nevertheless the dimensions are different. Rearranging the sensitivity matrix and heat flux vector, in Eq. (11), the future temperatures can be written as:

$$\begin{bmatrix} \mathbf{T}_{1\,\mathrm{fut}} \\ \vdots \\ \mathbf{T}_{J\,\mathrm{fut}} \end{bmatrix} = \begin{bmatrix} \mathbf{H}_{11} & \cdots & \mathbf{H}_{1P} & \mathbf{X}_{11\,\mathrm{fut}} & \cdots & \mathbf{X}_{1P\,\mathrm{fut}} \\ \vdots & \ddots & \vdots & \vdots & \ddots & \vdots \\ \mathbf{H}_{J1} & \cdots & \mathbf{H}_{JP} & \mathbf{X}_{J1\,\mathrm{fut}} & \cdots & \mathbf{X}_{JP\,\mathrm{fut}} \end{bmatrix} \begin{bmatrix} \hat{\mathbf{q}}_{1\,\mathrm{past}} \\ \vdots \\ \hat{\mathbf{q}}_{P\,\mathrm{past}} \\ \mathbf{q}_{1\,\mathrm{fut}} \\ \vdots \\ \mathbf{q}_{P\,\mathrm{fut}} \end{bmatrix} + \begin{bmatrix} \mathbf{T}_{10\,\mathrm{fut}} \\ \vdots \\ \mathbf{T}_{J0\,\mathrm{fut}} \end{bmatrix} \tag{13}$$

that is,

$$\mathbf{T}_{\mathrm{fut}} = [\mathbf{H}]\hat{\mathbf{q}}_{\mathrm{past}} + [\mathbf{X}_{\mathrm{fut}}]\mathbf{q}_{\mathrm{fut}} + \mathbf{T}_{0\,\mathrm{fut}} \tag{14}$$

where the vectors are:

$$\mathbf{T}_{\mathrm{fut}} = (\mathbf{T}_{1\,\mathrm{fut}}, \mathbf{T}_{2\,\mathrm{fut}}, \ldots, \mathbf{T}_{j\,\mathrm{fut}}, \ldots, \mathbf{T}_{J\,\mathrm{fut}})^T \tag{15a}$$

$$\hat{\mathbf{q}}_{\mathrm{past}} = (\hat{\mathbf{q}}_{1\,\mathrm{past}}, \hat{\mathbf{q}}_{2\,\mathrm{past}}, \ldots, \hat{\mathbf{q}}_{P\,\mathrm{past}})^T \tag{15b}$$

$$\mathbf{q}_{\mathrm{fut}} = (\mathbf{q}_{1\,\mathrm{fut}}, \mathbf{q}_{2\,\mathrm{fut}}, \ldots, \mathbf{q}_{P\,\mathrm{fut}})^T \tag{15c}$$

and the matrices are:

$$[\mathbf{H}] = \begin{bmatrix} \mathbf{H}_{11} & \mathbf{H}_{12} & \cdots & \mathbf{H}_{1P} \\ \mathbf{H}_{21} & \mathbf{H}_{22} & \cdots & \mathbf{H}_{2P} \\ \vdots & \vdots & \ddots & \vdots \\ \mathbf{H}_{J1} & \mathbf{H}_{J2} & \cdots & \mathbf{H}_{JP} \end{bmatrix} \tag{15d}$$

$$[\mathbf{X}_{\mathrm{fut}}] = \begin{bmatrix} \mathbf{X}_{11\,\mathrm{fut}} & \mathbf{X}_{12\,\mathrm{fut}} & \cdots & \mathbf{X}_{1P\,\mathrm{fut}} \\ \mathbf{X}_{21\,\mathrm{fut}} & \mathbf{X}_{22\,\mathrm{fut}} & \cdots & \mathbf{X}_{2P\,\mathrm{fut}} \\ \vdots & \vdots & \ddots & \vdots \\ \mathbf{X}_{J1\,\mathrm{fut}} & \mathbf{X}_{J2\,\mathrm{fut}} & \cdots & \mathbf{X}_{JP\,\mathrm{fut}} \end{bmatrix} \tag{15e}$$

In Eq. (14) the previous history is stored in [**H**] matrix and $\hat{\mathbf{q}}_{\mathrm{past}}$ vector. The vectors and matrix related with future temperatures are $\mathbf{T}_{\mathrm{fut}}$, $\mathbf{q}_{\mathrm{fut}}$ and $[\mathbf{X}_{\mathrm{fut}}]$.

Taking into account Eq. (14), the expression $[\mathbf{H}]\hat{\mathbf{q}}_{\mathrm{past}} + \mathbf{T}_{0\,\mathrm{fut}}$ can be interpreted as the calculated temperature over $t_{m-1} < t \leqslant t_{m+r-1}$, considering that in this time interval the input is held at zero. This concept is noted as:

$$[\mathbf{H}]\hat{\mathbf{q}}_{\mathrm{past}} + \mathbf{T}_{0\,\mathrm{fut}} = \mathbf{T}|_{\mathbf{q}\,\mathrm{fut}=0} \tag{16}$$

Finally, Eq. (14) can be written more compactly as:

$$\mathbf{T}_{\mathrm{fut}} = [\mathbf{X}_{\mathrm{fut}}]\mathbf{q}_{\mathrm{fut}} + \mathbf{T}|_{\mathbf{q}\,\mathrm{fut}=0} \tag{17}$$

This matrix equation is known as the standard form for the linear IHCP [6]. Notice that Eq. (17) can be applied to both one-dimensional and two-dimensional linear problems. However, the structure of each vector and each matrix is remarkably more complex for two-dimensional problems.

Again, the first attempt in order to solve the inverse problem, now in a sequential form, can be the identification of measured temperatures Y_{ji} with the calculated temperatures T_{ji}, expressed by Eq. (17), so that, assuming $J = P$, it is possible to obtain $\mathbf{q}_{\mathrm{fut}}$ vector from:

$$\mathbf{q}_{\mathrm{fut}} = [\mathbf{X}_{\mathrm{fut}}]^{-1}(\mathbf{Y}_{\mathrm{fut}} - T|_{\mathbf{q}\,\mathrm{fut}=0}) \tag{18}$$

We note that diagonal coefficients of each $[\mathbf{X}_{jk\,\mathrm{fut}}]$ lower triangular sub-matrix, in Eq. (15e), are equal to $\Delta\phi_{kj0}$. For the same reasons exposed above, this means that $[\mathbf{X}_{\mathrm{fut}}]$ can be an ill-conditioned matrix. Consequently, Eq. (18) is not recommended for resolving the IHCP in a sequential form. Therefore, an adequate stabilization technique is needed.

3.2. 2D linear IHCP based on sequential SVD

In a similar way to FSM, the sequential algorithm SVD uses r future temperatures (measured and calculated). Nevertheless, the stabilization technique is not based on the temporary specification of the unknown surface heat flux over r future time steps. For each $\mathbf{q}_k$ vector, it is assumed that components: $\hat{q}_{k1}, \hat{q}_{k2}, \ldots, \hat{q}_{k(m-1)}$, have been previously estimated (they are noted with "$\hat{}$"), and the objective is the estimation of the components q_{km} for $k = 1, 2, \ldots, P$, corresponding to the m-time step.

Now, in order to get a stable algorithm, the singular value decomposition (SVD) [12] of the small sensitivity matrix, $[\mathbf{X}_{\text{fut}}]$, will be considered, so that this matrix can be expressed as:

$$[\mathbf{X}_{\text{fut}}] = [\mathbf{U}][\mathbf{S}][\mathbf{V}]^T \tag{19}$$

where $[\mathbf{U}]$ and $[\mathbf{V}]$ are orthogonal matrices which column vectors are the eigenvectors of $[\mathbf{X}_{\text{fut}}] \cdot [\mathbf{X}_{\text{fut}}]^T$ and $[\mathbf{X}_{\text{fut}}]^T \cdot [\mathbf{X}_{\text{fut}}]$ respectively. These vectors will be noted as $\mathbf{u}_i$ and $\mathbf{v}_i$, and are called left and right singular vectors of $[\mathbf{X}_{\text{fut}}]$. The diagonal matrix $[\mathbf{S}] = \text{diag}[\lambda_1, \lambda_2, \ldots, \lambda_M]$ contains the square root of the eigenvalues of $[\mathbf{X}_{\text{fut}}] \cdot [\mathbf{X}_{\text{fut}}]^T$. These coefficients (noted as λ_i) are arranged in decreasing magnitude and are called the singular values of $[\mathbf{X}_{\text{fut}}]$. The factorization given by Eq. (19) can be expressed as an outer product expansion [20]:

$$[\mathbf{X}_{\text{fut}}] = [\mathbf{U}][\mathbf{S}][\mathbf{V}]^T = \sum_{i=1}^{J\times r} \lambda_i \mathbf{u}_i \mathbf{v}_i^T \tag{20a}$$

where

$$\mathbf{v}_i = (v_{1i}, v_{2i}, \ldots, v_{(J\times r)i})^T \tag{20b}$$

$$\mathbf{u}_i^T = (u_{1i}, u_{2i}, \ldots, u_{(J\times r)i}) \tag{20c}$$

In this expression, it has been assumed that $J = P$. Then the square matrix $[\mathbf{X}_{\text{fut}}]$, in Eq. (19), of rank $J \times r$ and dimension $(J \times r) \times (J \times r)$, has been decomposed as the sum of $J \times r$ matrices of rank 1 and dimension $(J \times r) \times (J \times r)$. This expansion is known as *Spectral decomposition*. The factorization SVD presents important properties, as well as outstanding interpretations and applications. One of the most interesting applications, in the ill-posed problems in order to get a reduced model, is based on reduced rank approximations. If expansion represented by Eq. (20a) is truncated to the p-first singular values and the corresponding left and right singular vectors (truncated SVD), the new matrix and the corresponding factorization (noted by the subscript $_{\text{red}}$) will be expressed as:

$$[\mathbf{X}_{\text{red}}] = [\mathbf{U}_{\text{red}}][\mathbf{S}_{\text{red}}][\mathbf{V}_{\text{red}}]^T = \sum_{i=1}^{p} \lambda_i \mathbf{u}_i \mathbf{v}_i^T, \quad p < J \times r \tag{21}$$

Golub and Van Loan [12] show that $[\mathbf{X}_{\text{red}}]$ is the closest matrix to $[\mathbf{X}_{\text{fut}}]$ that has rank p. With an adequate effective rank p, the approximation of $[\mathbf{X}_{\text{fut}}]$ by $[\mathbf{X}_{\text{red}}]$ presents a notable advantage in order to solve an inverse problem. Therefore, the matrix $[\mathbf{X}_{\text{red}}]$ will be considered, and with an adequate p-value, a stable algorithm is obtained:

$$\hat{\mathbf{q}}_{\text{fut}} = [\mathbf{X}_{\text{red}}]^{-1} (\mathbf{Y}_{\text{fut}} - \mathbf{T}|_{\mathbf{q}\,\text{fut}=0}) \tag{22}$$

where

$$[\mathbf{X}_{\text{red}}]^{-1} = [\mathbf{V}_{\text{red}}][\mathbf{S}_{\text{red}}]^{-1}[\mathbf{U}_{\text{red}}]^T = \sum_{i=1}^{p} \frac{1}{\lambda_i} \mathbf{v}_i \mathbf{u}_i^T, \quad p < J \times r \tag{23}$$

According to Eqs. (22), (23), the sequential SVD algorithm presents two tunable hyperparameters: r and p. For a given p-value, we can carry out numerical experiments in order to find the corresponding optimum r-value (r_{opt}). This optimum value is obtained from the minimization of the total error S, given by Eq. (29b). Note that great p-values require larger optimal r-values. This fact represents a disadvantage in an on-line process, because the time period $r_{\text{opt}} \cdot \Delta t$ (named as "look ahead" [21]) can be excessively long.

Assuming that SVD can be calculated numerically with an efficient code [22], it is possible to obtain a very simple algorithm. For a given p-value, Eq. (22) is reduced to:

$$\hat{\mathbf{q}}_{\text{fut}} = \sum_{i=1}^{p} \mathbf{v}_i \frac{1}{\lambda_i} \mathbf{u}_i^T (\mathbf{Y}_{\text{fut}} - \mathbf{T}|_{\mathbf{q}\,\text{fut}=0}) \tag{24}$$

where

$$\hat{\mathbf{q}}_{\text{fut}} = (\hat{\mathbf{q}}_{1\,\text{fut}}, \hat{\mathbf{q}}_{2\,\text{fut}}, \ldots, \hat{\mathbf{q}}_{P\,\text{fut}})^T \tag{25a}$$

with

$$\hat{\mathbf{q}}_{k\,\text{fut}} = (\hat{q}_{km}, \hat{q}_{k(m+1)}, \ldots, \hat{q}_{k(m+r-1)})^T \tag{25b}$$

Taking into account the sequential characteristic of this method, only the first components $\hat{q}_{km}$ with $k = 1, 2, \ldots, P$ (and it has been assumed that $J = P$) are retained. This calculus process is repeated for the next time step. Finally, from Eq. (24), the sequential SVD algorithm can be expressed more explicitly as:

$$\hat{q}_{km} = \sum_{i=1}^{p} v_{(k-1)\cdot r+1,i} \frac{1}{\lambda_i} \sum_{j=1}^{J\times r} u_{ji} (\mathbf{Y}_{\text{fut}} - \mathbf{T}|_{\mathbf{q}\,\text{fut}=0})_j \tag{26}$$

3.3. 2D non-linear IHCP based on sequential SVD

The quasi-linear approximation proposed by Beck et al. [6,10], in order to solve efficiently the IHCP using the FSM, can also be used for the sequential-in-time procedure, presented above, because the standard form of equations for linear IHCP, Eq. (17), is valid for both future temperature methods. This results in an efficient method (the computer time is substantially reduced) because iteration is not required for non-linear problems. The quasi-linearization is not possible to carry out on the whole domain methods.

In a sequential procedure, it is assumed that the surface heat flux components, $\hat{q}_{k(m-1)}$ with $k = 1, 2, \ldots, P$ (and with $J = P$) have been previously estimated at time t_{m-1}. In order to estimate $\hat{q}_{km}$ with $k = 1, 2, \ldots, P$ (and $J = P$) at time t_m, the linearization is introduced by evaluation of the thermal properties at time t_{m-1}, so that the properties are held constant over a reduced number (r) of future time steps, (t_m, t_{m+r-1}), which are used for the estimation of the surface heat flux components, $\hat{q}_{km}$ with $k = 1, 2, \ldots, P$ ($J = P$) at time t_m. This assumption implies a temporal linearization of the non-linear problem.

With the assumption given above, the future temperatures for $i = 1, 2, \ldots, r$, can be expressed in a linear form as:

$$T_{j(m+i-1)}(\mathbf{q}_{\text{fut}}) = T_{j(m+i-1)}(\mathbf{q}^*_{\text{fut}}) + \sum_{k=1}^{P} \sum_{n=1}^{i} \Delta\phi_{kj(i-n)} (q_{k(m+n-1)} - q^*_{k(m+n-1)}) \tag{27a}$$

where $\Delta\phi$ is the pulse sensitivity coefficient, which is defined as:

$$\Delta\phi_{kj(i-n)} = \frac{\partial T_{j(m+i-1)}}{\partial q_{k(m+n-1)}} \tag{27b}$$

and $\mathbf{q}^*_{\text{fut}}$ is an initial heat flux vector, which can be an arbitrary vector. However, $\mathbf{q}^*_{\text{fut}} = \mathbf{0}$ is a common choice. The corresponding response vector (natural response) will be noted as $\mathbf{T}(\mathbf{q}^*_{\text{fut}} = \mathbf{0}) = \mathbf{T}|_{\mathbf{q}\,\text{fut}=0}$. Considering the matrix form of Eq. (27a) the future temperatures can be expressed as:

$$\mathbf{T}(\mathbf{q}_{\text{fut}}) = \mathbf{T}_{\text{fut}} = \mathbf{T}|_{\mathbf{q}\,\text{fut}=0} + [\mathbf{X}_{\text{fut}}]\mathbf{q}_{\text{fut}} \tag{28}$$

It can be seen that Eq. (28) is equivalent to Eq. (17). This matrix equation represents the Duhamel integral in a discrete form, which is extended to r future time steps from the last estimated component. The same procedure mentioned in the previous subsection, can be applied now to Eq. (28), so that after considering the SVD of the sensitivity matrix $[\mathbf{X}_{\text{fut}}]$ (ill-conditioned) and the closest matrix of reduced rank $[\mathbf{X}_{\text{red}}]$ (well-conditioned), the same Eq. (24) is obtained. For that reason, Eq. (24) also can be used to solve non-linear problems, but it is important to remark that $\mathbf{T}|_{\mathbf{q}\,\text{fut}=0}$ and $[\mathbf{X}_{\text{fut}}]$ must be updated in each time interval considered.

The expression $\mathbf{T}|_{\mathbf{q}\,\text{fut}=0}$ can be calculated over $t_{m-1} < t \leqslant t_{m+r-1}$, solving a temperature direct problem and considering that in this time interval the input is held at zero. The initial condition corresponding to this direct problem is the temperature field at time t_{m-1}, $\hat{\mathbf{T}}_{m-1}$. According to the quasi-linear approximation, the thermal properties k, ρ and c are evaluated at the temperature at time t_{m-1}, and they are held constant for the r future time steps. Consequently, no iteration is required for the calculation of $\mathbf{q}_{\text{fut}}$.

Eq. (24) represents the solution of the system of algebraic equations for the estimation of the unknown parameters. Only the first components $\hat{q}_{km}$ with $k = 1, 2, \ldots, P$ (and it has been assumed that $J = P$), corresponding to the first time step, are retained from the solution given by Eq. (24). Then, time index is increased by one and the solution process is repeated by marching in time (updating the thermal properties at each time step) until the last time step is reached (the last components are estimated).

To use this inverse method, it is necessary to obtain values of the sensitivity coefficients. For linear problems (temperature-independent thermal properties) the sensitivity coefficients are the same for each analysis time interval, therefore, sensitivity coefficients are computed only once (for the first time interval). In non-linear problems (temperature-dependent thermal properties) the sensitivity matrix $[\mathbf{X}_{\text{fut}}]$ is found with the thermal properties fixed using the temperature field at the previous time step, t_{m-1}, but in the next time interval analysis $[\mathbf{X}_{\text{fut}}]$ must be updated.

It is well known that the sensitivity coefficients can be found using the sensitivity equations [10] or a finite difference approximation. In this paper, the sensitivity equation method is used, because it is typically more accurate and less unstable than the finite difference method [10,23]. There are P ($J = P$) sensitivity problems, and each of them is exactly the same as the direct problem in Eqs. (1a)–(1d) with the following simplifications: the initial condition in Eq. (1d) is zero, the heat flux $q(r, z, t)$ in Eq. (1b), taking into account Eq. (5), is replaced by the basis function $\Phi_k(s)$ with $k = 1, 2, \ldots, P$ ($J = P$) and the known boundary condition in Eq. (1c) is homogeneous ($T_\infty = 0$). The numerical computations for the sensitivity coefficients are also simplified because the matrices corresponding to the finite element formulation (the conductivity matrix and the capacitance matrix) do not change over r future time steps and they are the same as for the temperature problem.

4. Numerical results

In an IHCP there are two sources of error in the estimation. The first source is the unavoidable bias deviation (or deterministic error). The second source of error is the variance due to the amplification of measurement errors (stochastic error). The global effect of deterministic and stochastic errors is considered in the mean squared error or total error when only one parameter is estimated, S_k with $k = 1, 2, \ldots, P$. S_k is defined by:

$$S_k = \left[\frac{1}{N-1} \sum_{i=1}^{N} (\hat{q}_{ki} - q_{ki})^2 \right]^{1/2}, \quad 1 \leqslant k \leqslant P \tag{29a}$$

where N is the total number of estimated values corresponding to the kth parameter, $\hat{q}_{ki}$ is the estimated kth component at t_i and q_{ki} is the true value.

In addition, as the inverse problem usually involves the estimation of P parameters ($P > 1$), in this study an overall estimate, S, for the error has been defined as:

$$S = \left[\frac{1}{P} \sum_{k=1}^{P} S_k^2 \right]^{1/2} \tag{29b}$$

The overall estimate, S, considers the total error, S_k, of each parameter estimated, $k = 1, 2, \ldots, P$.

The value of the estimate, S, defined in Eq. (29b), is used to decide when the best estimation of the surface heat flux has been reached, so that the optimization criterion is the minimization of S. The value of S_k provides information about the accuracy of the estimation reached in an only point in the space (space position which corresponds to the location of the kth parameter). By contrast, S provides information of the estimation on the complete surface, since this one considers all the points of the surface (set of points in which the parameters must be estimated). Therefore, the idea is not to try the minimization of the total error of each parameter, but to minimize the total error of the estimations of all the parameters simultaneously. This criterion will be very useful in this comparative study.

It must be pointed out that sequential algorithms (FSM and SVD) use r measurements before heating starts ($t < 0$). In accordance with Beck et al. [6], this is performed in order to minimize the effect of the anomalous calculation during the first few steps.

The sample problem is illustrated in Fig. 1. An axisymmetric cylinder wall $ABCD$ ($R_1 = 0.5$ m, $R_2 = 1.5$ m, $AC = BD = 1$ m, $AB = CD = R_1 - R_2 = 1$ m) is composed of a material with the following thermal properties: the volumetric heat capacity has been considered constant ($c = 1$ J kg^{-1} °C^{-1}, $\rho = 1$ kg m^{-3}) for the linear problem, as well as the thermal conductivity ($k = 1$ W m^{-1} °C^{-1}), whereas for the non-linear problem it has been considered the following temperature dependence: $k = 1 + T$ W m^{-1} °C^{-1}. This wall is subjected to a heat flux imposed on side AC, and three convective boundary conditions relative to a fluid temperature $T_\infty = 0$ °C ($h = 1$ W m^{-2} °C^{-1} on AB, on BD and on CD). Temperature measurements are taken from two sensors located at a distance of 0.5 m from AC as is shown in Fig. 1. The two unknown heat flux components on AC are placed at the corners. The goal is to estimate the heat flux components on AC using the temperature measurements.

Firstly, several direct problems have to be solved. In order to obtain the simulate temperature data using the FEM formulation, the domain is modelled with a regular mesh (648 triangular elements and 361 nodes). The same spatial mesh is used in order to calculate the sensitivity coefficients. We notice that in the inverse analysis, the boundary corresponding to unknown heat flux (AC in Fig. 1) is discretized with only two degrees of freedom. By contrast, the same boundary contributes with 19 nodes to the mesh used on the direct problems. On the other hand, direct problems are solved considering a high temporal resolution. The time-stepping considered is based on backward difference. This scheme is pure implicit and unconditionally stable. It is evident that time-step size required by the inverse algorithm is significantly larger than the one used in direct problems. If Δt_D and Δt_I represent the time step used in the direct and inverse problems, the values of the ratio $\Delta t_I / \Delta t_D$ were the following: 100, 50 and 25. The great differences between the discretization used in direct and inverse problems, avoid the problem named as "inverse crime". The expression "inverse crime" is used to denote the act of employing the same model to generate, as well as to invert, synthetic data.

For each inverse method we have considered: four shapes of the input as shown in Fig. 2, with two different levels of error in temperature measurements and three sizes of time step in each case (0.1 s, 0.05 s and 0.025 s). In addition, linear and non-linear

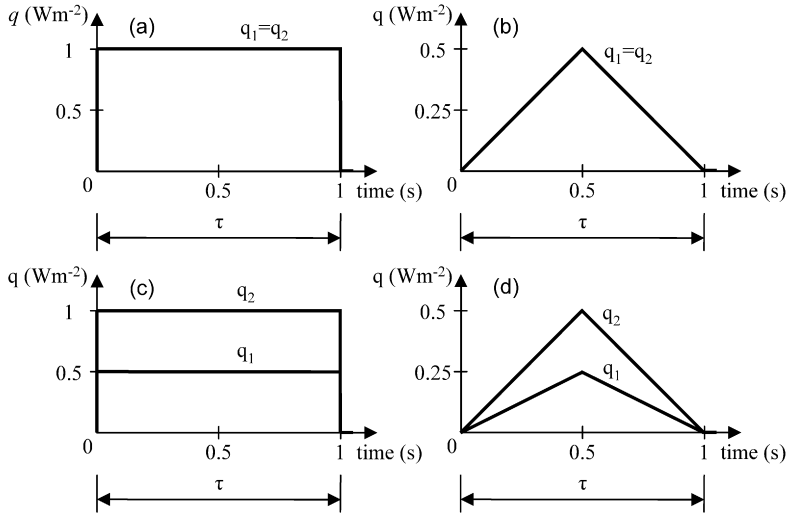

Fig. 2. Shapes of the heat flux considered in the sample problem.

problems are studied. This implies a total of 48 cases. Tables 1 and 2 summarize the results corresponding to the best estimation obtained by FSM and sequential SVD (noted as SSVD) in all cases considered. Each case taken into account appears in a row, while the following information is represented in columns: test used, level of error in temperature measurements (σ), size of the time step (Δt), method used (FSM or SSVD), optimum p-value (in SSVD only), optimum r-value, overall estimate of error (S) and number case.

It can be appreciated that two levels of measurement noises, $\sigma = 0.001\,^{\circ}\mathrm{C}$ and $\sigma = 0.005\,^{\circ}\mathrm{C}$, have been considered for the rectangular tests, which correspond to Figs. 2(a) and 2(c). Taking as reference the maximum increase of temperature (0.157 °C) at location sensor for the linear problem, and considering (around the exact temperatures) an error range between $\pm 2.576\sigma$ (or 99% confidence interval), these noise levels (low and high) correspond to error percentages of 1.64% and 8.20% respectively for the linear problem. In the same way, the levels of measurement noises considered for the triangular tests, which correspond to Figs. 2(b) and 2(d), have been $\sigma = 0.001\,^{\circ}\mathrm{C}$ and $\sigma = 0.002\,^{\circ}\mathrm{C}$. These noise levels correspond to error percentages of 5.05% and 10.10% respectively.

Firstly, the linear problem will be considered, and secondly, the non-linear problem. In Table 1, the results obtained in all cases considered for the linear problem are summarized. Comparing the overall error estimates (S), the results obtained by the two sequential procedures are very similar. The SSVD algorithm provides slightly more accurate results in most cases considered in this study (24 comparisons altogether), except in three of them (comparison of cases 31–32, 37–38 and 43–44 in Table 1). Considering the tests represented in Figs. 2(a) and 2(b), $p = 1$ has been the optimum p-value (reduced rank) found for the SSVD method. The SSVD algorithm is slightly superior to the FSM in all these cases (12 comparisons altogether, cases 1–24 in Table 1). Note that the optimum r-value (number of future temperatures) is similar in both sequential methods, but in SSVD algorithm it is always smaller or equal to FSM, except only in one case (comparison of cases 19–20 in Table 1) that corresponds to test showed in Fig. 2(b): high level of noise in temperature measurements ($\sigma = 0.002\,^{\circ}\mathrm{C}$), and low temporal resolution ($\Delta t = 0.1$ s). For this reason (relatively large time step), the best estimation requires a small number of future temperatures: $r = 2$ in the FSM and $r = 3$ in the SSVD method. This results contrast with the previous studies about the one-dimensional problem [19] where the optimum r-value required by FSM and SSVD is the same in all cases considered. Taking into account the tests represented in Figs. 2(c) and 2(d), the optimum reduced rank is $p = 3$ for the SSVD method in these cases (12 comparisons altogether, cases 25–48 in Table 1). Now, comparing the tabulated results, the SSVD algorithm provides slightly more accurate results than the FSM in all cases considered, except in the three mentioned above (comparison of cases 31–32, 37–38 and 43–44 in Table 1), which always correspond to a low temporal resolution, and hence, to a low optimum r-value. However, the optimum r-value in SSVD algorithm is always greater or equal to the one in FSM.

The estimated heat flux computed using FSM and SSVD is shown in Fig. 3 as an example for the linear problem. This example (comparisons of cases 15–16 and 21–22 in Table 1) considers the effect of noise level in measurement errors through a triangular test (Fig. 2(b)). Two levels (low and high) of noise measurements $\sigma = 0.001\,^{\circ}\mathrm{C}$ and $\sigma = 0.002\,^{\circ}\mathrm{C}$ are considered. In both comparisons, the time step has been $\Delta t = 0.05$ s. Due to its size, twenty measurements ($N = 20$) are included in the interval $\tau = 1$ s. Figs. 3(a) and 3(b) compare the results corresponding to the best estimation obtained by FSM and SSVD. If we had used errorless data (by setting $\sigma = 0$), it might be thought that inverse algorithm does not need any regularization, nevertheless the exact data are real numbers and they are limited by the number of significant digits of the computer. For this reason a weak regularization provides the optimal estimation in the most of cases. For example, if we consider errorless data, the same triangular test and the same time step ($\Delta t = 0.05$ s), the best estimation using FSM is obtained for $r = 2$ and the overall estimate of error is $S = 0.0036$. Notice that if the regularization is not considered ($r = 1$), the estimation is significantly worse ($S = 6.6309$). The best estimation using SSVD and errorless data is obtained for $p = 1$ and $r = 2$. The overall error is $S = 0.0104$. As it can be seen in Table 1, the estimations using errorless data are significantly superior to those obtained using data affected by errors.

Another example (comparisons of cases 25–26 and 29–30 in Table 1) that takes into account the effect of the time step size through a rectangular test (Fig. 2(c)) has been considered. The noise level has been $\sigma = 0.001\,^{\circ}\mathrm{C}$. The graphical representation corresponding to a case like this is shown in Fig. 4, which represents the best estimation obtained by both methods for the linear problem. Two sizes of the time step $\Delta t = 0.1$ s and $\Delta t = 0.025$ s are considered. Fig. 4(a) refers to a relatively large time step $\Delta t = 0.1$ s. Because of its size, only $N = 10$ measurements are included. Fig. 4(b) refers to a $\Delta t = 0.025$ s, so that $N = 40$.

Table 1
Comparison of error estimations for the linear IHCP in different cases

Test	σ (°C)	Δt (s)	Method	p_{opt}	r_{opt}	**S** (W m^{-2})	Case
Fig. 2(a)	0.001	0.1	FSM	–	1	0.0986	1
			SSVD	1	1	0.0511	2
		0.05	FSM	–	2	0.1314	3
			SSVD	1	2	0.1224	4
		0.025	FSM	–	3	0.1344	5
			SSVD	1	3	0.1206	6
	0.005	0.1	FSM	–	2	0.2160	7
			SSVD	1	2	0.1902	8
		0.05	FSM	–	5	0.2178	9
			SSVD	1	3	0.1766	10
		0.025	FSM	–	6	0.2110	11
			SSVD	1	4	0.1660	12
Fig. 2(b)	0.001	0.1	FSM	–	2	0.0347	13
			SSVD	1	2	0.0316	14
		0.05	FSM	–	4	0.0337	15
			SSVD	1	3	0.0237	16
		0.025	FSM	–	6	0.0300	17
			SSVD	1	6	0.0215	18
	0.002	0.1	FSM	–	2	0.0632	19
			SSVD	1	3	0.0429	20
		0.05	FSM	–	5	0.0465	21
			SSVD	1	3	0.0343	22
		0.025	FSM	–	9	0.0472	23
			SSV	1	7	0.0258	24
Fig. 2(c)	0.001	0.1	FSM	–	1	0.1009	25
			SSVD	3	2	0.0694	26
		0.05	FSM	–	2	0.1148	27
			SSVD	3	3	0.1011	28
		0.025	FSM	–	4	0.1138	29
			SSVD	3	7	0.0982	30
	0.005	0.1	FSM	–	2	0.1883	31
			SSVD	3	3	0.2258	32
		0.05	FSM	–	5	0.1771	33
			SSVD	3	6	0.1603	34
		0.025	FSM	–	7	0.1788	35
			SSVD	3	10	0.1597	36
Fig. 2(d)	0.001	0.1	FSM	–	2	0.0343	37
			SSVD	3	3	0.0469	38
		0.05	FSM	–	4	0.0313	39
			SSVD	3	6	0.0298	40
		0.025	FSM	–	7	0.0281	41
			SSVD	3	9	0.0257	42
	0.002	0.1	FSM	–	2	0.0630	43
			SSVD	3	3	0.0824	44
		0.05	FSM	–	5	0.0462	45
			SSVD	3	6	0.0426	46
		0.025	FSM	–	9	0.0440	47
			SSVD	3	11	0.0421	48

Later, a graphical representation of the singular values of the sensitivity matrix $[\mathbf{X}_{fut}]$ (Eq. (15e)) and the corresponding Condition Number (CN, ratio between largest and smallest singular values) are considered. They give a good insight about the degree of ill-posedness of the inverse problem. Furthermore, a clear justification of the optimum values of hyperparameters p and r of Eq. (24) is obtained. The approximation of $[\mathbf{X}_{fut}]$ (of rank $(J \times r)$ and dimension $(J \times r) \times (J \times r)$) by $[\mathbf{X}_{red}]$ (of rank p and dimension $(J \times r) \times (J \times r)$) presents a notable advantage in order to solve an inverse problem. The elimination of $(J \times r) - p$ smallest terms of Eq. (20a) has a negligible effect on a direct problem, but it can be strictly necessary in an inverse problem, in order to reduce the CN and the numerical instability.

The following cases have been selected: 16, 22, 26 and 30 of Table 1. The corresponding representation is showed in Fig. 5. In cases 16 and 22, the sensitivity matrix $[\mathbf{X}_{fut}]$ is the same, because in both cases the time step, the optimum values of r and p are the same. Nevertheless, the estimations are different because noise level (σ) is higher in case 22. Fig. 5(a) shows the singular values of the sensitivity matrix for these cases. The corresponding

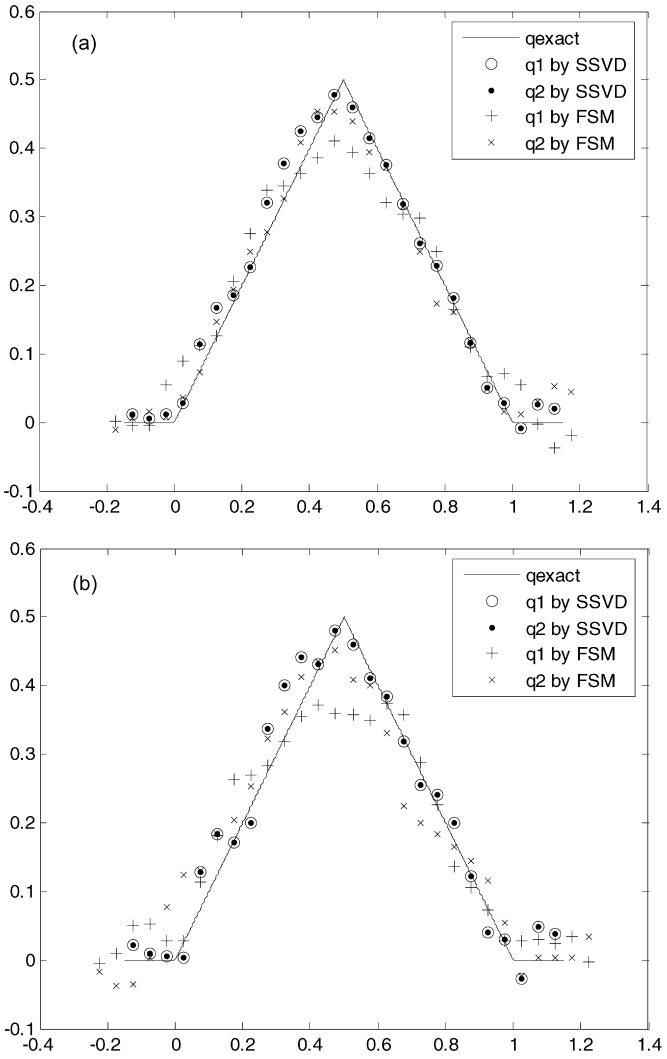

Fig. 3. Estimated heat flux in the linear problem for $\Delta t = 0.05$ s (a) for $\sigma = 0.001$ °C (cases 15, 16 in Table 1) and (b) for $\sigma = 0.002$ °C (cases 21, 22 in Table 1).

CN = 24.86. In all cases, the objective is to estimate two parameters ($J = 2$), but the triangular test corresponding to cases 16 and 22 uses identical parameters ($q_1 = q_2$). Consequently, the information provided by each sensor (symmetrically located) is the same. For this reason $p_{opt} = 1$. Notice that in this case, the maximum simplification of the system provides the optimal estimation and the condition number of matrix $[\mathbf{X}_{red}]$ is CN = 1.

Figs. 5(b) and 5(c) correspond to singular values of the sensitivity matrix of cases 26 and 30, respectively. In both cases, the rectangular test uses different parameters ($q_1 \neq q_2$), and the information provided by each sensor is equally different. In case 26, the size of time step is relatively large ($\Delta t = 0.1$ s). This implies that the singular values are also relatively large. However, CN is not too large (CN = 5.62). For this reason, the optimum r-value requires only two future temperatures and the dimension of sensitivity matrix is 4×4. The best estimation is obtained for $p = 3$, and the condition number of matrix $[\mathbf{X}_{red}]$ is CN = 3.47. This implies that it is only necessary to remove the last singular value (and the corresponding singular vectors).

Next, the process of finding the optimal parameters is considered in this example. Firstly, in order to analyze the maximum simplification of the system, a reduced rank $p = 1$ is considered. This simplification involves only one degree of freedom, and only one parameter can be estimated. The only one parameter esti-

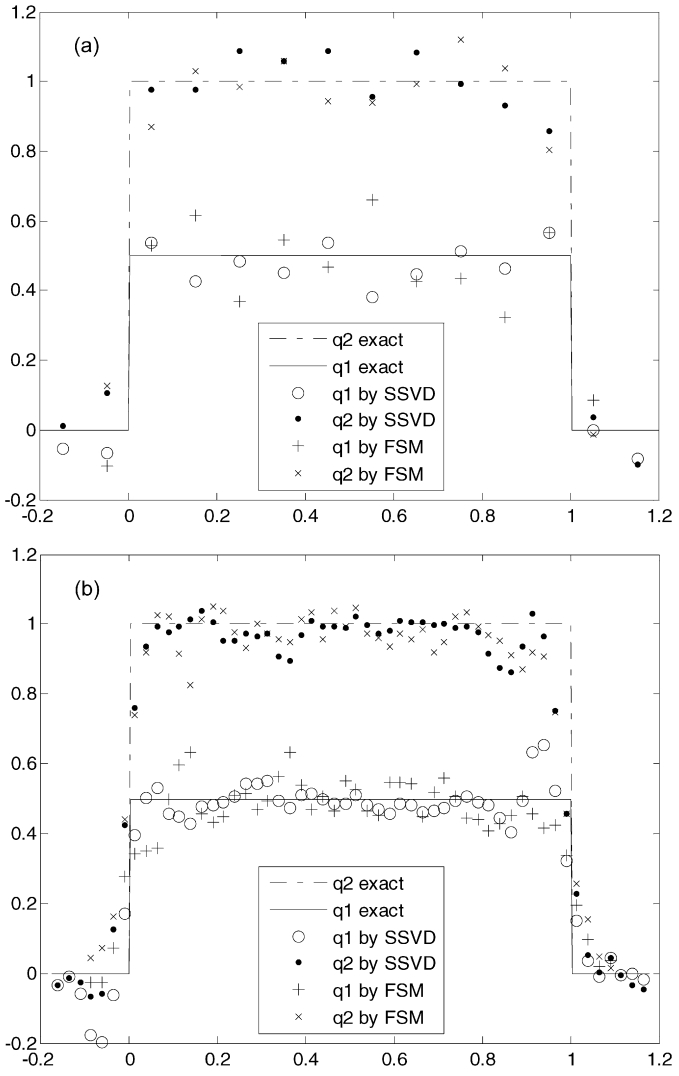

Fig. 4. Estimated heat flux in the linear problem for $\sigma = 0.001\,^{\circ}\mathrm{C}$ (a) for $\Delta t = 0.1$ s (cases 25, 26 in Table 1) and (b) for $\Delta t = 0.025$ s (cases 29, 30 in Table 1).

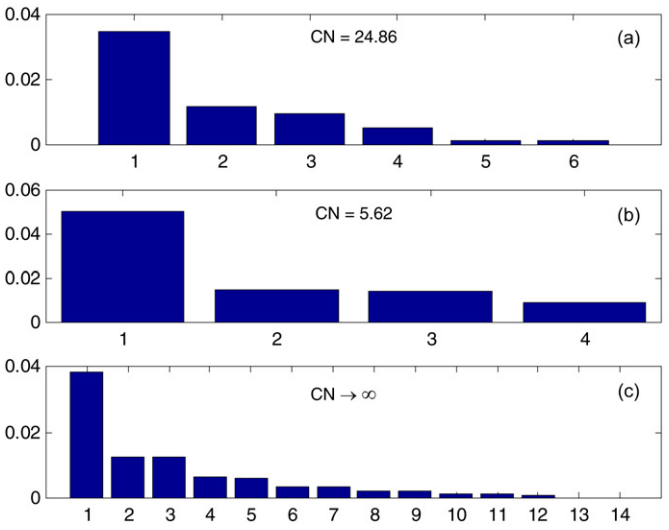

Fig. 5. Graphical representation of the singular values and CN of the sensitivity matrix corresponding to cases 16, 22, 26 and 30 of Table 1.

mated oscillates around the average value of q_1 and q_2. For example, if we consider $p = 1$, the overall error estimate for $r = 1$ and $r = 2$ is $S = 0.2442$ and $S = 0.2549$, respectively. Obviously, the condition number of matrix $[\mathbf{X}_{\mathrm{red}}]$ is $\mathrm{CN} = 1$ in both estimations. Next, we consider $p = 2$. The overall error estimate for $r = 1$ and $r = 2$ is $S = 0.1009$ and $S = 0.2177$ respectively, and the corresponding condition number of matrix $[\mathbf{X}_{\mathrm{red}}]$ is $\mathrm{CN} = 2.4265$ and $\mathrm{CN} = 3.3311$. If we consider $p = 3$, it is not possible to use $r = 1$ with two parameters ($J = 2$). This is because the dimension of $[\mathbf{X}_{\mathrm{fut}}]$ is 2×2. Using $r = 2$ and $r = 3$, the overall error estimate and the condition number of the reduced matrix are $S = 0.0694$, $S = 0.1143$, $\mathrm{CN} = 3.4690$ and $\mathrm{CN} = 4.2625$, respectively. Finally, if we consider $p = 4$, the overall error estimate and the condition number of the reduced matrix for $r = 2$ and $r = 3$ are $S = 0.0762$ and $S = 0.0860$, $\mathrm{CN} = 5.6500$ and $\mathrm{CN} = 5.7797$, respectively. Notice that for a given value of p, the optimal r-value corresponds with the minor CN. Consequently, for the test corresponding to solid line of Fig. 2(c), with a time step $\Delta t = 0.1$ s and a noise level $\sigma = 0.001\,^{\circ}\mathrm{C}$, the best estimation corresponds to $p_{\mathrm{opt}} = 3$ and $r_{\mathrm{opt}} = 2$. Fig. 5(b) shows that second and third singular values of $[\mathbf{X}_{\mathrm{fut}}]$ are equal, consequently if $r = 2$, it is not surprising that $p_{\mathrm{opt}} = 3$.

Furthermore, it is clear that the degree of ill-posedness of case 26 is low. By contrast, case 30 is an example of severe ill-posed problem. As expected, this case requires much more information of future temperatures, $r_{\mathrm{opt}} = 7$ and the dimension of sensitivity matrix is 14×14. Fig. 5(c) shows singular values. As the smallest singular value tends to zero, CN tends to infinity. This is because in this case, the size of time step ($\Delta t = 0.025$ s) is four times smaller than in case 26. Again, the best estimation is obtained for $p = 3$, and the condition number of matrix $[\mathbf{X}_{\mathrm{red}}]$ is $\mathrm{CN} = 3.05$. Notice that, in all cases of Table 1 corresponding to tests using two different parameters, the optimum p-value is equal to three.

In all cases considered, the two sensors are symmetrically located. In order to get the greatest possible degree of independence between the two sensors, they are located to the greatest possible distance between them (see Fig. 1). Also notice that both sensors are located at the same distance of the heated surface. If a sensor is placed at a greater distance than the rest, more remote sensors do not add significant information [6].

Following, the non-linear problem is analyzed. Similar conclusions are obtained for the non-linear problem. Table 2 summarizes the results obtained in all the cases considered. Comparing the overall error estimates (S), the results obtained by the two sequential procedures are similar. The SSVD algorithm provides slightly more accurate results in most cases, except in four of them (comparison of cases 31–32, 33–34, 37–38 and 43–44 in Table 2). Taking into account the tests represented in Figs. 2(a) and 2(b), $p = 1$ has been the optimum p-value found for the SSVD method. The SSVD algorithm is slightly superior to the FSM in all these cases (12 comparisons altogether, cases 1–24 in Table 2). In addition, the optimum r-value in SSVD algorithm is also always smaller or equal to that in FSM, except in one case (comparison of cases 19–20 in Table 2) that corresponds to the test showed in Fig. 2(b): high level of noise in temperature measurements ($\sigma = 0.002\,^{\circ}\mathrm{C}$) and low temporal resolution ($\Delta t = 0.1$ s). Viewing the tests represented in Figs. 2(c) and 2(d), the optimum reduced rank is $p = 3$ for the SSVD method in these cases (12 comparisons altogether, cases 25–48 in Table 2). Now, comparing the tabulated results, the SSVD algorithm provides slightly more accurate results than the FSM in all cases considered, except in the four mentioned above (comparison of cases 31–32, 33–34, 37–38 and 43–44 in Table 2), which correspond to a low temporal resolution. However, the optimum r-value in SSVD algorithm is always greater or equal to the one in FSM.

Graphical representations of the best estimation of heat flux versus time are plotted in Fig. 6 as an example (comparisons of

Table 2
Comparison of error estimations for the non-linear IHCP in different cases

Test	σ (°C)	Δt (s)	Method	p_{opt}	r_{opt}	**S** (W m^{-2})	Case
Fig. 2(a)	0.001	0.1	FSM	–	1	0.0913	1
			SSVD	1	1	0.0368	2
		0.05	FSM	–	2	0.1318	3
			SSVD	1	2	0.1260	4
		0.025	FSM	–	3	0.1295	5
			SSVD	1	2	0.1151	6
	0.005	0.1	FSM	–	2	0.2209	7
			SSVD	1	2	0.1934	8
		0.05	FSM	–	5	0.2238	9
			SSVD	1	3	0.1796	10
		0.025	FSM	–	5	0.2135	11
			SSVD	1	4	0.1608	12
Fig. 2(b)	0.001	0.1	FSM	–	2	0.0355	13
			SSVD	1	2	0.0327	14
		0.05	FSM	–	4	0.0346	15
			SSVD	1	3	0.0245	16
		0.025	FSM	–	6	0.0304	17
			SSVD	1	6	0.0223	18
	0.002	0.1	FSM	–	2	0.0636	19
			SSVD	1	3	0.0445	20
		0.05	FSM	–	5	0.0474	21
			SSVD	1	3	0.0345	22
		0.025	FSM	–	9	0.0482	23
			SSVD	1	6	0.0263	24
Fig. 2(c)	0.001	0.1	FSM	–	1	0.0939	25
			SSVD	3	2	0.0681	26
		0.05	FSM	–	2	0.1146	27
			SSVD	3	3	0.0987	28
		0.025	FSM	–	4	0.1150	29
			SSVD	3	7	0.1009	30
	0.005	0.1	FSM	–	2	0.1893	31
			SSVD	3	3	0.2227	32
		0.05	FSM	–	5	0.1805	33
			SSVD	3	5	0.1830	34
		0.025	FSM	–	7	0.1817	35
			SSVD	3	10	0.1633	36
Fig. 2(d)	0.001	0.1	FSM	–	2	0.0348	37
			SSVD	3	3	0.0470	38
		0.05	FSM	–	4	0.0318	39
			SSVD	3	6	0.0301	40
		0.025	FSM	–	6	0.0284	41
			SSVD	3	9	0.0261	42
	0.002	0.1	FSM	–	2	0.0631	43
			SSVD	3	3	0.0823	44
		0.05	FSM	–	5	0.0468	45
			SSVD	3	6	0.0423	46
		0.025	FSM	–	9	0.0447	47
			SSVD	3	11	0.0425	48

cases 3–4 and 9–10 in Table 2) for the non-linear problem. In these comparisons, the effect of noise level in measurement errors has been considered using the test showed in Fig. 2(a). The time step has been $\Delta t = 0.05$ s, and this value implies $N = 20$. Two levels of noise measurements $\sigma = 0.001\,^{\circ}\mathrm{C}$ and $\sigma = 0.005\,^{\circ}\mathrm{C}$ have been considered. The thermal conductivity varies almost 50% during the simulated experiment, which has a maximum temperature change of 0.4902 °C. Although this variation is not typical of most materials, it provides a stringent test for the method and linearization procedure.

Another example is illustrated in Fig. 7 (comparisons of cases 37–38 and 41–42 in Table 2) which considers the effect of the time step size using the test showed in Fig. 2(d) for the non-linear problem. Two sizes of the time step $\Delta t = 0.1$ s and $\Delta t = 0.025$ s are considered and, in both cases, the noise level $\sigma = 0.001\,^{\circ}\mathrm{C}$ has been considered. Figs. 7(a) and 7(b) compare the results corresponding to the best estimation obtained by FSM and SSVD. In these cases, the maximum temperature change is 0.1455 °C, which implies a variation of 14.5% of the thermal conductivity.

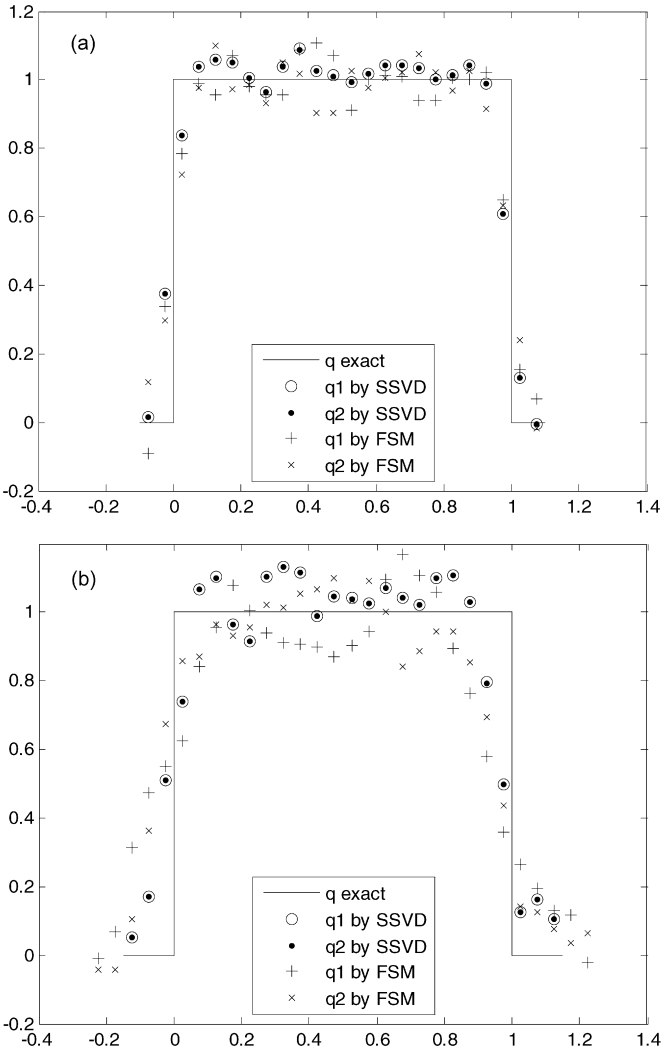

Fig. 6. Estimated heat flux in the non-linear problem for $\Delta t = 0.05$ s (a) for $\sigma = 0.001\,^{\circ}\mathrm{C}$ (cases 3, 4 in Table 2) and (b) for $\sigma = 0.005\,^{\circ}\mathrm{C}$ (cases 9, 10 in Table 2).

It should be noted that in cases where the two parameters must be equal ($q_1 = q_2$, in the tests corresponding to Figs. 2(a) and 2(b)) the estimations provided by SSVD are biased but they are quasi-equal ($\hat{q}_1 \cong \hat{q}_2$). By contrast, the corresponding estimations provided by FSM are biased but they are clearly unequal ($\hat{q}_1 \neq \hat{q}_2$). This fact can be seen in Fig. 3 for the linear problem and in Fig. 6 for the non-linear problem. As the temperature measurements are simulated (in each sensor location) with different random noises (but with the same σ), this means that the FSM is more sensitive to random noise of measurements than the SSVD algorithm. This justifies the slight superiority of the SSVD method in these cases.

Finally, a comparison between the computing time of FSM and SSVD algorithms is considered. For this purpose, we have selected a total of eight cases of Table 2, which correspond to non-linear inverse problems. The methods were implemented using MATLAB v6.5. The CPU timings were obtained using a Pentium 4 CPU, 2.66 GHz computer with 248 MB of RAM. Table 3 summarizes the CPU time (in seconds), required by each method. Column "ratio" contains ratios between CPU time of FSM and CPU time of SSVD, for each case considered. As can be seen in Table 3, the number of future temperatures r is the most influential parameter in the CPU time. Notice that when the optimum r-value is the same in both methods (cases 3 and 4), the CPU time is very similar. This shows that the computing time required by the factorization SVD of the small sensitivity matrix is not significant.

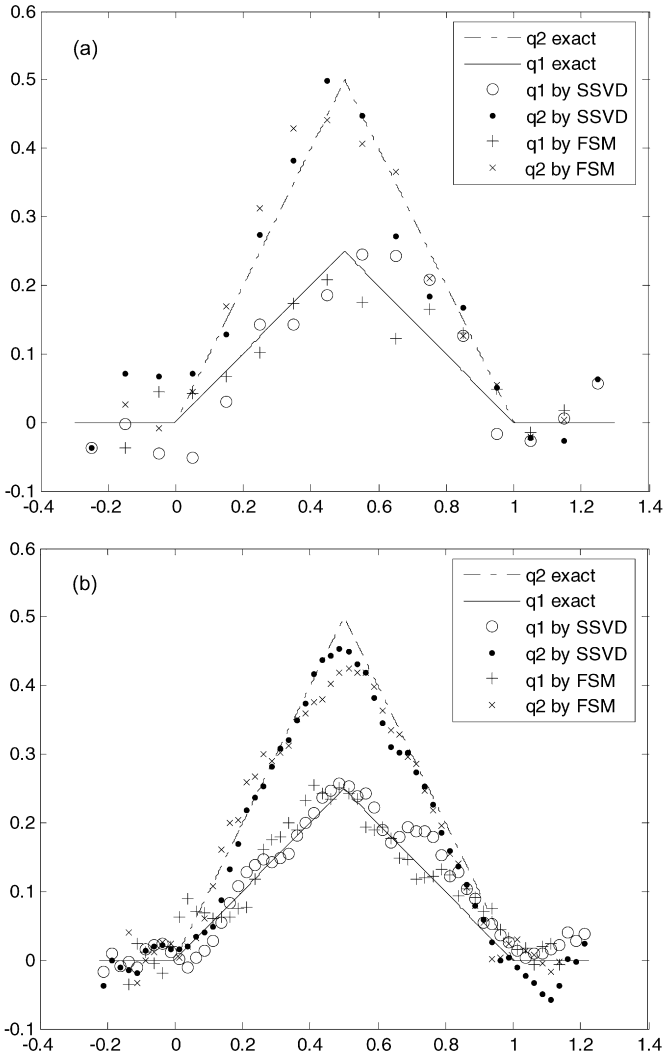

Fig. 7. Estimated heat flux in the non-linear problem for $\sigma = 0.001\,^{\circ}\mathrm{C}$ (a) for $\Delta t = 0.1$ s (cases 37, 38 in Table 2) and (b) for $\Delta t = 0.025$ s (cases 41, 42 in Table 2).

5. Summary and conclusions

In this paper, a sequential estimation method is presented for the solution of a general two-dimensional and non-linear inverse heat conduction problem (IHCP). The regularization procedure used for the solution of the IHCP is based on the singular value decomposition (SVD) technique of the small sensitivity matrix. The inverse algorithm has been implemented in conjunction with the finite element method (FEM) and can be applied in two-dimensional planar or cylindrical axisymmetric geometries.

The estimation of an unknown surface heat flux implies the estimation of a set of temporal functions corresponding to spatial nodes on the surface of the body. In general, the number of surface nodes is very large. To reduce the number of unknown heat flux components to be estimated, a parameterization of the spatial distribution of the unknown surface heat flux is used. This method has been accomplished considering that the number of parameters (heat flux components to estimate) is equal to the number of temperature sensors.

The sequential-in-time SVD algorithm (SSVD) allows a quasi-linear approximation in the calculations of the temperatures and sensitivity coefficients (the thermal properties were held constant during the calculations in each analysis interval). This conceptually results in an efficient sequential method (substantial reduction of the computer time), because this procedure eliminates iterations and reduces the calculations necessary for the reformulation of the finite element conductivity and capacitance matrices.

Table 3
CPU times of FSM and SSVD algorithms for the non-linear IHCP in several different cases (Table 2)

Test	σ (°C)	Δt (s)	Method	CPU time (s)	Ratio	Case
Fig. 2(a)	0.001	0.05	FSM	524.5	0.97	3
			SSVD	539.6		4
	0.005	0.05	FSM	1631.9	1.93	9
			SSVD	846.9		10
Fig. 2(d)	0.001	0.1	FSM	607.2	0.58	37
			SSVD	1039.0		38
	0.001	0.025	FSM	1716.0	0.60	41
			SSVD	2869.3		42

The results show that this method does not require a priori information for the functional form of the unknown quantities to perform the inverse calculations.

Test cases presented verify the application and the stability of the method. In addition, the accuracy of the scheme presented was evaluated by comparison with Function Specification Method (FSM). This comparative study was carried out using numerically simulated data, and the parameters considered were the following: the shape of the input, the noise level of measurement, the size of time step and the temperature-dependent thermal properties. An overall estimate of error has been defined in order to find the optimal estimation of the surface heat flux in the two-dimensional IHCP. In general, the FSM and SSVD algorithm give similar results, and the surface heat flux was reasonably reproduced. However, SSVD algorithm provides slightly more accurate results than the FSM in most cases considered. Moreover, the optimum r-value (optimal number of future temperatures) required by SSVD algorithm is smaller or equal to the one in FSM in many cases (where only one parameter must be considered on the active surface). The opposite occurs when several parameters are estimated.

Acknowledgements

This work is supported in part by a grant from the Andalusian Government through P.A.I. (Group TEP-157). The authors thank Ms. M. Molina Gutiérrez for her improvement of the English text. Finally, the authors are very grateful for the useful comments and suggestions offered by reviewers.

References

[1] O.V. Nagornov, Yu.V. Konovalov, V.S. Zagorodonov, L.G. Thompsom, Reconstruction of the surface temperature of artic glaciers from the data of temperature measurement, J. Eng. Phys. Thermophys. 74 (2001) 253–265.
[2] M. Janicki, M. Zubert, A. Napieralski, Application of inverse problem algorithms for integrated circuit temperature estimation, Microelectronic J. 30 (1999) 1099–1107.
[3] F. Rosa, A. Valverde, J.M. Aranda, J. Aranda, J. Rodríguez, CESA-1 Project capabilities for high temperature material testing: Application to the Hermes wing leading edge tests, Solar Energy 46 (1991) 175–182.
[4] T.G. Kim, Z.H. Lee, Time-varying heat transfer coefficients between tube-shaped casting and metal mold, Int. J. Heat Mass Transfer 40 (1997) 3513–3525.
[5] J. Lin, Inverse estimation of the tool-work interface temperature in end milling, Int. J. Mach. Manufact. 35 (1995) 751–760.
[6] J.V. Beck, B. Blackwell, C.R. Clair St., Inverse Heat Conduction: Ill Posed Problems, Wiley-Interscience, New York, 1985.
[7] A.N. Tikhonov, V.Y. Arsenin, Solution of Ill-Posed Problems, V.H. Winston & Sons, Washington, DC, 1977.
[8] O.M. Alifanov, Inverse Heat Transfer Problems, Springer, New York, 1994.
[9] D.A. Murio, The Mollification Method and the Numerical Solution of Ill-Posed Problems, Wiley-Interscience, New York, 1993.
[10] A.M. Osman, K.J. Dowding, J.V. Beck, Numerical solution of the general two-dimensional inverse heat conduction problem (IHCP), J. Heat Transfer 119 (1997) 38–45.

[11] K.J. Dowding, J.V. Beck, A sequential gradient method for the inverse heat conduction problems, J. Heat Transfer 121 (1999) 300–306.
[12] G.H. Golub, C.F. Van Loan, Matrix Computations, John Hopkins Univ. Press, Baltimore, 1983.
[13] T.J. Martin, G.S. Dulikravich, Inverse determination of boundary conditions and sources in steady heat conduction with heat generation, J. Heat Transfer 118 (1996) 546–554.
[14] T.J. Martin, G.S. Dulikravich, Inverse determination of steady heat convection coefficient distributions, J. Heat Transfer 120 (1998) 328–334.
[15] S.-Y. Shen, A numerical study of inverse heat conduction problems, Comput. Math. Appl. 38 (1999) 173–188.
[16] W.B. Muniz, F.M. Ramos, F. De Campos, Entropy and Tikhonov-based regularization techniques applied to the backwards heat equation, Comput. Math. Appl. 40 (2000) 1071–1084.
[17] J.R. Shenefelt, R. Luck, R.P. Taylor, J.T. Berry, Solution to inverse heat conduction problems employing singular value decomposition and model-reduction, Int. J. Heat Mass Transfer 45 (2002) 67–74.
[18] G.L. Lagier, H. Lemonnier, N. Coutris, A numerical solution of the linear multidimensional unsteady inverse heat conduction problem with the boundary element method and the singular value decomposition, Int. J. Thermal Sci. 43 (2004) 145–155.
[19] J.M. Gutiérrez, J.A. Martín, A. Corz, A sequential algorithm of inverse heat conduction problems using singular value decomposition, Int. J. Thermal Sci. 44 (2005) 235–244.
[20] D. Kalman, A singularly valuable decomposition: The SVD of a matrix, The American University, Washington, DC 20016, 2002.
[21] K.A. Woodbury, S.K. Thakur, Redundant data, future times and sensor location in the inverse heat conduction problem: A case study, Inverse Problems Engrg. Mech. 2 (1994) 193–199.
[22] W.H. Press, S.A. Teukolsky, W.T. Vetterling, B.P. Flannery, Numerical Recipes in Fortran, Cambridge University Press, 1992.
[23] J.V. Beck, K.J. Arnold, Parameter Estimation in Engineering and Science, Wiley, New York, 1977.